Physics of the Earth and Planetary Interiors, 36 (1984) 285–290
Elsevier Science Publishers B.V., Amsterdam – Printed in The Netherlands

Mantle flow due to internal vertical forces

J.F. Harper

Department of Mathematics and Institute of Geophysics, Victoria University of Wellington, Wellington (New Zealand)

(Received November 17, 1983; revision accepted May 17, 1984)

Harper, J.F., 1984. Mantle flow due to internal vertical forces. Phys. Earth Planet. Inter., 36: 285–290.

Morgan's and Blake and Chwang's image system gives the flow due to a point force in a viscous fluid in the neighbourhood of a plane rigid wall. I show that it can provide a good simple approximation for the flow in the Earth's mantle and the forces on the surface plates in two cases of geophysical interest: the uplift associated with cessation of subduction, and the "ridge push" driving mechanism for plate tectonics. For the latter case the method overcomes difficulties due to Gibbs' phenomenon in the alternative method of Fourier analysis. The method also predicts the distortion of a sinking slab detached from its oceanic plate if the viscosities in it and outside it are the same, but viscosity contrasts are more likely to make the conclusions unreliable than in the other cases.

1. Introduction

The Earth's mantle flows like a Newtonian viscous fluid under the action of sufficiently small stresses exerted for sufficiently long periods of time (see, for example, Parsons and Richter, 1981). The variation of viscosity with depth is not well known, and we ignore it in the interests of mathematical simplicity. Our results will therefore not be applicable to the real Earth in quantitative details but it is hoped that they are qualitatively interesting. I use as a model for the mantle a spherical shell of uniform viscosity with a rigid upper boundary (the plates) and a tangentially stress-free lower boundary (the core). Plate motions are ignored, as the purpose of this work is to study flows due to density inhomogeneities in the mantle; if desired, flow due to plate motions could be superposed on those found herein, because the governing equations are linear.

Inhomogeneities in density give rise to vertical forces, by Archimedes' principle. I investigate simple approximations to the flow due to those forces, using the Stokes flow image theories of Collins (1958), Morgan (1965), Blake and Chwang (1974) and Harper (1983). The results are used to estimate the amount of uplift which should occur at the surface when a subduction zone ceases subducting beneath. On calculating the flow induced in the mantle, I find that much of the flattening at the bottom of old detached subducted slabs, e.g., Tonga and the New Hebrides (Barazangi et al., 1973) would occur even in a constant-viscosity mantle. It does not require high viscosity at or beneath the bottoms of the slabs.

The method also allows me to re-derive Hager and O'Connell's (1981) theory for the forces involved in their form of the "ridge push" mechanism for oceanic plate propulsion, by a method which is not only simpler than theirs but also free of Gibbs' phenomenon.

2. Vertical Stokeslets and their images

Stokes' stream function ψ for the flow of an unbounded fluid of dynamic viscosity η due to a point force F at the origin of a spherical polar coordinate system (r, θ) is well known to be the "Stokeslet" solution (Batchelor, 1967)

$$\psi = (F/8\pi\eta) r \sin^2\theta \qquad (1)$$

if the force is along the axis of symmetry from $\theta = 0$ towards $\theta = \pi$, and the velocity components

0031-9201/84/$03.00

(v_r, v_θ) are given by

$$v_r = -(1/r \sin\theta)\partial\psi/\partial\theta$$

$$v_\theta = (1/r \sin\theta)\partial\psi/\partial r$$

The image systems for Stokeslets near spherical rigid boundaries have been described by Oseen (1927), Collins (1958), Usha (1980) and Usha and Nigam (1983). For spherical free boundaries the theory is due to Harper (1983) if the Stokeslet is vertical.

For my present applications of the theory, I need to consider only image systems for a force F applied close to a rigid outer surface, say within 0.1 Earth radii of it, and at a much greater distance from the free core boundary (i.e., at least 0.355 Earth radii or 0.65 core radii, as the core radius is 0.545 of the Earth's). Harper's (1983) theory then showed that if one wished to know viscous stresses at the outer surface, neglecting the images in the core would cause errors of a few per cent at most. Henceforth I shall do so. In addition, the viscous stresses can be shown to fall off rapidly at distances from a Stokeslet greater than its depth. As we are considering only shallow Stokeslets, we can ignore curvature of the Earth as well as the presence of the core, to a first approximation.

The image systems then reduce to those of Morgan (1965) and Blake and Chwang (1974), who calculated them for plane boundaries. In Cartesian coordinates (x, y, z), where the interior of the Earth is $z > 0$, and the Stokeslet is at $(0, 0, h)$, the surface stresses are

$$p_{zz} = 3Fh^3/2\pi r_1^5 \tag{2}$$

$$(p_{xz}, p_{yz}) = \nabla\left(Fh^2/2\pi r_1^3\right) = -\left(3Fh^2/2\pi r_1^5\right)(x, y) \tag{3}$$

where r_1 is, the distance from the Stokeslet to $(x, y, 0)$, i.e. $(x^2 + y^2 + h^2)^{1/2}$.

A simple case of considerable geophysical interest is a long horizontal line distribution of Stokeslets. This is used below in modelling dipping slabs and aging oceanic plates. If the vertical force per unit length is f, and the line is $x = 0$, $z = h$, then simple integrations of eqs. 2 and 3 lead to

$$p_{zz} = 2fh^3/\pi R^4 \tag{4}$$

$$p_{xz} = \nabla\left(fh^2/\pi R^2\right) = -2fh^2x/\pi R^4 \tag{5}$$

$$p_{yz} = 0 \tag{6}$$

where $R^2 = x^2 + h^2$. The stresses on the surface are thus strongly concentrated towards the line directly above the line Stokeslet, though less so than for a point Stokeslet, because of the inverse fourth power law replacing the inverse fifth power law with distance from it.

The normal stress eqs. 2 and 4 indicate that the surface would be depressed above a downward force in the mantle, and raised above an upward one. The shear stress potential in eq. 5 shows that if a plate boundary occupies the line $x = y = 0$ directly above the line Stokeslet, the plates on each side will be pushed apart by a force $-f/\pi$ per unit length of strike, f being positive for a downward Stokeslet (for which the plates are attracted towards it) and negative for an upward one.

The result $-f/\pi$ is independent of the viscosity, but it holds accurately only if the viscosity is uniform in a half-space below the surface. Variable viscosities or different geometries imply factors other than $-1/\pi$ multiplying f above. For example, if the viscosity were uniform in the region between two parallel rigid planes, a Stokeslet near the upper plane would give a result close to $-1/\pi$ but a Stokeslet near the lower plane would give a result close to zero, as its image in that plane has a small far field. There is an extensive mathematical literature on problems of this kind; see Liron and Mochon (1976) for the flow due to an individual Stokeslet, and Spence (1983) and Harper and Wake (1983) for eigenfunction expansions and how to evaluate them numerically.

3. Consequences

3.1. *Post-subduction uplift*

As an application of the theory in section 2, consider a subducted slab, of density higher than the surrounding mantle's, which is no longer attached to an oceanic plate and is sinking under its own weight deeper into the mantle. Because the maximum normal stress at the surface is $2f/\pi h$ from eq. 4, as h increases the stress decreases.

While subduction continues, the Earth's surface sinks under the action of the stress to a depth d given by

$$d = 2f/\pi\rho gh \qquad (7)$$

if the trough thereby created were empty, where ρ is the density of upper mantle rock, i.e., ~ 3.3 g cm^{-3}, and g is the acceleration due to gravity. If, instead, the trough filled up to the previous ground level with sediment of density ρ_s, then d would be multiplied by the usual isostatic factor $\rho/(\rho - \rho_s)$ (see Holmes, 1965, p. 1123).

For a slab, of course, one must not just use the line-force formulae (4) or (7), but integrate with them over the region occupied at depth by material of excess density. According to Ringwood (1982), a slab has ~ 6 km of eclogite with excess density of 0.15 g cm^{-3} overlying 23.5 km of harzburgite with 0.03 g cm^{-3}. In addition the 40 km of pyrolite beneath that will average some 500°C cooler than normal mantle, and so be 0.05 g cm^{-3} denser. The total mass anomaly is thus $\sim 3.62 \times 10^6$ kg m^{-2} in the slab. This figure can also be estimated (Hager and O'Connell, 1981) by considering isostasy in the oceanic plate; their result is higher by a factor of 2.35. Disagreements by factors of this order are typical of theories for mantle properties based on different kinds of data!

If we treat the slab as a plane distribution between 80 and 400 km depth, integration gives the results shown in Fig. 1 for three different dip angles: 30°, 60°, and 90°. The maximum value of p_{zz} turns out (on Ringwood's theory for the mass anomaly) to be 364 bar for vertical dip, corresponding to a trough 1.4 km deep if full of air, 2 km if full of water ($\rho_s = 1$ g cm^{-3}) or 5 km if full of sediment with $\rho_s = 2.4$ g cm^{-3}. Figure 1 shows that reducing the angle of dip makes little difference to this maximum depth, but spreads the trough out over a broader area on its inland side. If we use Hager and O'Connell's mass anomaly instead of Ringwood's, the trough depths become

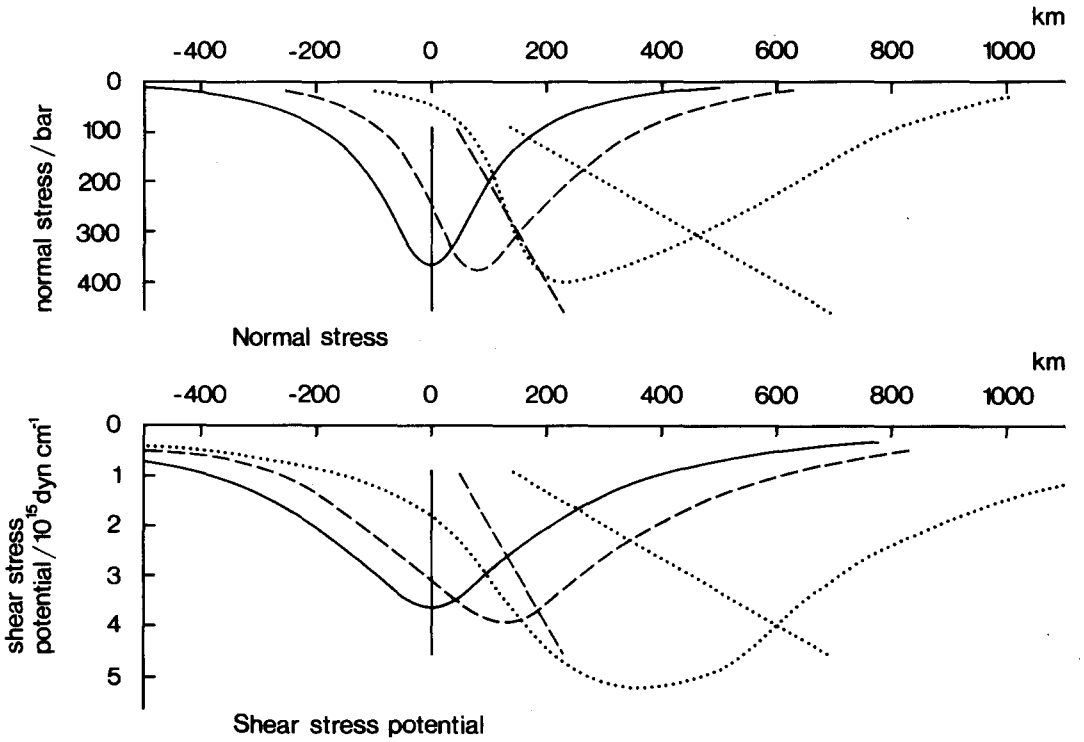

Fig. 1. Graphs of normal stress p_{zz} (upper graphs) and shear stress potential $\int p_{xz} dz$ (lower graphs) against distance perpendicular to the strike of subduction zones in the positions shown. Solid curves: vertical dip (90°). Dashed curves: 60° dip. Dotted curves: 30° dip.

3.3, 5 and 12 km, respectively.

Perhaps the most interesting consequence of eq. 7 is that if the subduction ceases, f will decrease slightly owing to heat diffusion through the Earth's surface (though diffusion inside the Earth leaves the total Stokeslet strength unchanged), and h will increase as it sinks deeper, on time-scales of 10 Ma or so. The dynamic support for the trough then disappears, and it will be uplifted, by the same amount as the preceding subsidence by the time any sedimentary fill has been eroded away, i.e., by up to 5 km on Ringwood's theory, or 12 km on Hager and O'Connell's. As such basins and uplifts are over many old subduction zones it appears that their formation could be largely due to viscous coupling to the slab via the mantle.

The maximum shear stress on the bottom of the surface plate is somewhat smaller than the normal stress. Integrating eq. 5 gives 102 bar (using Ringwood, 1982) or 240 bar (using Hager and O'Connell, 1981) for the vertical slab mentioned above, at 93 km either side of the line above it. There is a resultant horizontal force from either side towards this line of 3.6×10^{15} dyn cm^{-1} or 8.5×10^{15} dyn cm^{-1} for a vertical slab, and rather more for obliquely dipping ones. This "trench suction" is of the same order as the other forces driving the plates, though the shear stresses are not by themselves enough to break a plate: 102 bar (or 240 bar) are of the order of stress drops commonly found in earthquakes, but the strength of the lithosphere is much greater.

3.2. Distortion of slabs

Because Archimedes' principle implies that a slab of dense rock sinking in the mantle behaves like a distribution of Stokeslets, it is possible to calculate where those Stokeslets move to and thus how the slab distorts, if we assume that the viscosity is the same inside and outside the slab. In reality the viscosity inside it is higher; the effect of this will be that distortion is less pronounced in the real Earth than in the simplified model, but it should be in the same direction. We also make the simplifying approximations that the upper surface is flat and rigid, and that the core is far enough away to be unimportant, as before. Then the motion of a slab, from an initial position such as an elliptic cylinder with the cylinder axis horizontal and the major axis of the ellipse inclined, can be followed by calculating the velocity induced by a distribution of Stokeslets inside it, together with their images in the rigid upper surface. As time goes on, the Stokeslets are distributed inside the current position of the (by now distorted) cylinder. The results shown in Fig. 2 were obtained with a computer program due to Dr. K.M. Jansson (personal communication, 1983).

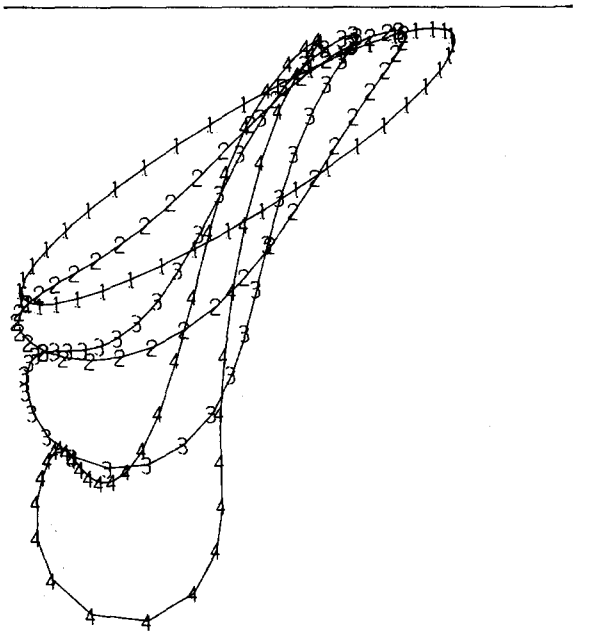

Fig. 2. The sequence of positions occupied at equal time intervals by a slab initially of elliptic cylindrical cross-section with major axis dipping 30° below the horizontal. Digits on the grid points indicate the time sequence; they follow the motion of individual points on the slab's surface.

Figure 2 shows, as would be expected, that the slab moves faster where it is further from the rigid upper boundary, and therefore it steepens. What was perhaps less expected is that it also thins at the top, becomes wider at the bottom, and curves up again near the tip. Physically, this last effect is because the induced downward velocity is greatest where the slab is fattest, and as that is not at the bottom end, that end will tend to be left behind. We conclude that distortions from planarity such as those found in the southwest Pacific (Barazangi et al., 1973) need not be due to inability to

penetrate a barrier at 650 km or thereabouts: similar distortions would happen even in a uniform mantle.

However, the viscosity is higher in real slabs than in the surrounding mantle. As a result, the distortions will be much less pronounced in the real Earth than in this simplified model of it (Whitehead and Luther, 1975).

3.3. *Ridge push*

"Ridge push" has been put forward by several authors, e.g., Lliboutry (1969), Artyushkov (1974), Harper (1975) and Lister (1975) as one of the forces driving plates. Lister (1975) showed that if the plate thickness varies as the square root of its age, with a density profile having the error-function profile expected of a thermal boundary layer to the asthenosphere beneath, and if astenosphere material becomes essentially rigid (and therefore forms part of the plate above) after a relatively small drop in temperature, then the hydrostatic pressure distribution on the plate gives rise to a horizontal force per unit area $\underset{\sim}{F}_A$ driving the plate away from the ridge, where

$$\underset{\sim}{F}_A = g\rho\gamma T_1 \kappa \nabla t \tag{8}$$

where g and ρ are as in section 3.1, γ is the coefficient of thermal expansion, T_1 is the temperature difference between asthenosphere and sea floor, κ the plate's thermal diffusivity and t its age. Lister (1975) obtained $|\underset{\sim}{F}_A| = 7.2$ bar from $\rho = 3.3$ g cm^{-3}, $\gamma = 4 \times 10^{-5}$ °C^{-1}, $T_1 = 1120$°C, $\kappa = 8 \times 10^{-3}$ cm^2 s^{-1}, and a half-spreading rate of 5 cm y^{-1} so that $|\nabla t| = 0.2$ y cm^{-1}.

More recently, Hager and O'Connell (1981) showed that if the cooled asthenosphere were assumed to be viscous instead of rigid, beneath a thin flat rigid lid, then a horizontal force per unit area $\underset{\sim}{F}_A$ would still be present, but now due to viscous shear on the underside of the plate. They found it to be of similar magnitude to Lister's, and approximately uniform away from plate boundaries.

I can use the theory developed in section 2 above to solve Hager and O'Connell's (1881) problem by a Green's function technique instead of a Fourier series, as follows. Imagine a 2-dimensional distribution of density anomaly, $\nabla\rho(x, z)$, where z measures depth below the rigid horizontal lid, in a fluid of uniform viscosity. By eq. 5 this induces a shear stress $\underset{\sim}{F}_A(x, 0)$ on the lid given by

$$\underset{\sim}{F}(x, 0) = \nabla \left[\iint \frac{g\Delta\rho(x_1, z) z^2 \mathrm{d}z\mathrm{d}x_1}{\pi\{(x - x_1)^2 + z^2\}} \right] \tag{9}$$

where the integration is over the region occupied by the density anomaly. The denominator in the integrand is small only where $|x - x_1|$ is of order z, and for a density distribution, such as is found beneath an oceanic plate, whose x-variation is on a length scale of thousands of kilometres but whose z-variation is on a scale of tens of kilometres, we can take x_1 as constant in $\nabla\rho(x_1, z)$ when doing the x_1 integration and obtain

$$\underset{\sim}{F}_A(x, 0) = \nabla \left(\int g\Delta\rho(x, z) z \mathrm{d}z \right) \tag{10}$$

If $\Delta\rho$ has Lister's (1975) error-function distribution

$$\Delta\rho = \rho\gamma T_1 \operatorname{erfc}\left(z / 2\sqrt{\{\kappa t\}}\right) \tag{11}$$

we recover the same results as eq. 8: not even a constant multiplier is different. Uniform viscosity is essential for this result; variation of viscosity with depth would modify it in ways which are hard to predict, except that a large rise in viscosity at the bottom of the asthenosphere would reduce the surface shear stresses slightly, for reasons given at the end of section 2.

It therefore does not matter whether the oceanic mantle lithosphere is taken to be a dense rigid body thickening with age or a viscous fluid whose upper dense part thickens with age: in either case a stress of the same magnitude and direction propels the plate away from the ridge. In obtaining both Lister's (1975) result and Hager and O'Connell's (1981), the chemical density contrasts were ignored; only those due to temperature differences were taken into account. The simplification introduces negligible error in the present problem, because the chemical stratification is horizontal for an oceanic plate. It needs to be considered only when the plate turns to dip steeply at a subduction zone.

4. Conclusions

(1) The known Green's function (Blake and Chwang, 1974) for the flow due to a vertical point force in a viscous fluid with a horizontal rigid boundary gives a good simple approximation for flow due to density inhomogeneities in the Earth's mantle if, as may well be the case, it is of nearly uniform viscosity. The Earth's core has negligible effects on the surface stresses due to forces applied within a few hundred kilometres of the surface.

(2) The viscous forces on the plate above a subduction zone cause it to sink several kilometres while the region above the slab fills up with sediment. It then rises a similar distance after the subduction stops, while the sediment erodes away.

(3) When the subduction stops and a slab sinks deeper, it would deform by thickening and flattening at the bottom even in a mantle of constant viscosity. The flattening observed at certain subduction zones is not by itself a proof of impenetrability of the layers beneath. These results will be modified if the viscosity is higher inside the slab, but no theory has yet shown how greatly.

(4) Ridge push can be calculated simply and analytically for a uniformly viscous oceanic lithosphere: a problem for which the previously available method required more extensive computation.

Acknowledgements

I thank Dr Kalvis Jansson for the use of his computer program for following the motion of distributions of Stokeslets, the Victoria University of Wellington for research and study leave, Wolfson College, Cambridge for a visiting fellowship, and the Department of Applied Mathematics and Theoretical Physics, Cambridge, for computing facilities and a congenial working environment while the first draft of this paper was being written.

References

Artyushkov, E.V., 1974. Can the Earth's crust be in a state of isostasy? J. Geophys. Res., 79: 741–752.

Barazangi, M., Isacks, B.L., Oliver, J., Dubois, J. and Pascal, G., 1973. Descent of lithosphere beneath New Hebrides, Tonga–Fiji and New Zealand. Nature, 242: 98–101.

Batchelor, G.K., 1967. An introduction to Fluid Dynamics. University Press, Cambridge, 615 pp.

Blake, J.R. and Chwang, A.T., 1974. Fundamental singularities of viscous flow. Part I: The image systems in the vicinity of a stationary no-slip boundary. J. Eng. Math., 8: 23–29.

Collins, W.D., 1958. Note on a sphere theorem for the axisymmetric Stokes flow of a viscous fluid. Mathematika, 5: 118–121.

Hager, B.H. and O'Connell, R.J., 1981. A simple global model of plate dynamics and mantle convection. J. Geophys. Res., 86: 4843–4867.

Harper, J.F., 1975. On the driving forces of plate tectonics. Geophys. J.R. Astron. Soc., 40: 465–474.

Harper, J.F., 1983. Axisymmetric Stokes flow images in spherical free surfaces with applications to rising bubbles. J. Aust. Math. Soc. (Ser. B), 25: 217–231.

Harper, J.F. and Wake, G.C., 1983. Stokes flow between parallel plates due to a transversely moving end wall. IMA J. Appl. Math., 30: 141–149.

Holmes, A., 1965. Principles of Physical Geology. Thomas Nelson, London and Edinburgh, 2nd edn., 1288 pp.

Liron, N. and Mochon, S., 1976. Stokes flow for a Stokeslet between two parallel flat plates. J. Eng. Math., 10: 287–303.

Lister, C.R.B., 1975. Gravitational drive on oceanic plates caused by thermal contraction. Nature, 257: 663–665.

Lliboutry, L., 1969. Sea floor spreading, continental drift and lithosphere sinking with an asthenosphere at melting point. J. Geophys. Res., 74: 6525–6540.

Morgan, W.J., 1965. Gravity anomalies and convection currents. I. A sphere and cylinder sinking beneath the surface of a viscous fluid. J. Geophys. Res., 70: 6175–6187.

Oseen, C.W., 1927. Neuere Methoden und Ergebnisse in der Hydrodynamik. Akademische Verlagsgesellschaft, Leipzig, 337 pp.

Parsons, B. and Richter, F.M., 1981. Mantle convection and the oceanic lithosphere. In: C. Emiliani (Editor), The Sea. Wiley-Interscience, New York, Vol. 7, pp. 73–117.

Ringwood, A.E., 1982. Phase transformations and differentiation in subducted lithosphere: implications for mantle dynamics, basalt petrogenesis, and crustal evolution. J. Geology, 90: 611–643.

Spence, D.A., 1983. A class of biharmonic end-strip problems arising in elasticity and Stokes flow. IMA J. Appl. Math., 30: 107–139.

Usha, R., 1980. Flow at small Reynolds numbers. Ph.D. thesis, Indian Institute of Technology, Madras, pp 4–17.

Usha, R. and Nigam, S.D., 1983. Flow in the asthenosphere — I (Axisymmetric problem). J. Math. Phys. Sci. (India), 17: 579–589.

Whitehead, J.A., Jr. and Luther, D.S., 1975. Dynamics of laboratory diapir and plume models. J. Geophys. Res., 80: 705–717.